IEEE Access
Multidisciplinary | Rapid Review | Open Access Journal

Received January 7, 2020, accepted February 4, 2020, date of publication February 11, 2020, date of current version February 20, 2020.

Digital Object Identifier 10.1109/ACCESS.2020.2973184

The Improved Constraint Methods for Foot-Mounted PDR System

WENCHAO ZHANG[1,2], DONGYAN WEI[1], AND HONG YUAN[1]
[1]Aerospace Information Research Institute, Chinese Academy of Sciences, Beijing 100094, China
[2]University of Chinese Academy of Sciences, Beijing 100094, China

Corresponding authors: Wenchao Zhang (zhangwenchao@aoe.ac.cn) and Dongyan Wei (weidy@aircas.ac.cn)

This work was supported by the National Key Research Program of China "Collaborative Precision Positioning Project" under Grant 2016YFB0501900.

ABSTRACT The Zero-velocity Update (ZUPT) aided Extended Kalman Filter (EKF) is commonly used in the classical INS-based foot-mounted PDR (Pedestrian Dead Reckoning) system. However, in the realistic test, the system still often suffers from drift, which is mainly caused by two reasons: failed detection of the stationary phase in the dynamic pedestrian gait and the heading drift which is a poorly observable variable of the ZUPT method. In this paper, in order to overcome these problems, three improved constraint algorithms have been proposed respectively for the detection of the stationary phase, constraint of heading drift and constraint of the height divergence. Firstly, for the problem of failed detection of the stationary phase, a novel stationary phase detection method is proposed which mainly by finding the minimum detector T in each gait cycle to determine the stationary phase, rather than totally based on threshold comparison principle in the traditional method. Comparing with the traditional method, the proposed method can detect the stationary phase of each gait cycle accurately under various pedestrian movements. Secondly, for the heading divergence problem, an improved method is proposed based on the existing HDE (Heuristic Drift Elimination) method, which uses the position error rather than heading error to restrain the trajectory divergence. Comparing with the traditional method, the proposed method can better constrain the heading to the correct angle. At last, for the problem of height divergence, an effective method has been proposed to determine the state of pedestrians by using the slope between adjacent one/several footsteps. At the same time, the slope of the plane and stairs is used to restrict the height divergence. In experiment, the proposed method can be more effectively to distinguish the pedestrian's state. Especially, when pedestrian walks on the stairs, the slope of the stairs can constrain the height divergence obviously.

INDEX TERMS ZUPT-aided EKF, stationary phase detection, improved HDE, slope detection, height constraint.

I. INTRODUCTION

The Global Navigation Satellite System (GNSS) is a basic pedestrian positioning method. However, in urban canyons and indoor environments, GNSS positioning systems cannot be used due to signal attenuation and interference. Indoor pedestrian positioning system is an effective means of indoor positioning, which is a good complement to the GNSS positioning system. Many scholars have proposed different methods for indoor pedestrian positioning system. Among these methods, the foot-mounted inertial measurement unit (IMU) has wide range of applications, due to its independence from pre-installed infrastructures [1], and it can independently implement pedestrian positioning.

Since the IMU always suffer from drift, the position, velocity and heading errors of the foot-mounted IMU grow with time. The Zero Velocity Updates (ZUPT) is a commonly used method to constrain the divergence of the inertial recursive positioning result. It assumes that during walking, the foot touches the ground and remains stationary for a short time (stance phase) [2]. However, when pedestrian under various pedestrian movements, most ZUPT methods usually can't effectively detect the stationary period. Meanwhile, the heading error during pedestrian movement is unobservable for ZUPT method [3], so, the ZUPT-assisted Extended Kalman Filter (EKF) algorithm is less restrictive to the

The associate editor coordinating the review of this manuscript and approving it for publication was Lubin Chang.

heading, which means the heading still will diverge with time.

The detection of the stance phase is a key step of the ZUPT method, and many detection methods have been developed [4]–[7]. Commonly-used detection methods include the acceleration magnitude method [8], the angular velocity magnitude method [9]–[12], the moving variance method [13], or a combination of the above methods [14], [15]. In addition, there are some other methods, such as, in [7], the zero-speed interval is determined based on a likelihood ratio test (LRT) detector. The detector provides good performance at low gait speeds (approximately 0.83 m/s). In [4], a segmentation based on the gyro output is used to construct a hidden Markov model-based algorithm. The algorithm exhibits good reliability under walking and running conditions. However, the state transition model is complex and difficult to implement. In [5], a standing phase detector consisting of a foot detector and two zero-speed detectors is proposed. The detector can successfully detect zero-speed during walking, climbing stairs and running. However, when pedestrians alternate between walking and running, the detectors are easily confused. All of these methods above basically have a common characteristic that the stationary phase detection is based on setting a threshold, by comparing the detector with the threshold to determine whether the current moment is in the stationary phase in the dynamic pedestrian gait. These methods have significant advantage when the pedestrian in the single motion, which means the magnitude of stationary phase detector basically kept within a stable range. However, in the case of movement including walking, running, upstairs and downstairs, etc., the zero-speed detection threshold fluctuates greatly with the movement condition, and these methods can't have a universally applicable threshold that can effectively detect the stationary phase under various pedestrian movements.

To suppress the heading drift, magnetic field is often used as a stable orientation reference. But the magnetic field inside buildings changes rapidly while space and time changes, and it is also sensitive to some metal objects or electrical equipment [16], [17]. As most buildings have regular structures, researchers proposed to use corridor's directions in buildings as constraints, which has been proved to be an effective method for the heading drift of INS (Inertial Navigation System)-based PDR system. For instance, Abdulrahim et al. [13] stressed that most of indoor corridors are in 4 major directions (called as dominant directions), either parallel or orthogonal to each other and to the peripheral walls of the building. They have developed Heuristic Drift Elimination (HDE) algorithm that corrects the computed heading by matching with the closest dominant direction. Then, the heading difference (heading error) between the dominant directions and the stride heading is fed as a measurement into the Kalman filter. When the Stride Length (SL) is shorter than 0.3 m, the heading correction is deactivated. It works well for short stretch of walking in non-dominant directions. But for prolonged walk in the non-dominant directions, the heading drift still will present. This method has been improved by Jimenez. A R to accommodate curved path in some special buildings and this improved method is called iHDE [18]. However, the HDE and iHDE methods both use the position (stride) heading between adjacent footsteps to determine whether pedestrian's walking direction closes to the indoor corridor heading (the dominant directions), and then use the heading difference between position heading and the closest reference corridor heading to correct the pedestrian current inertia recursive heading. Although, the reference corridor heading is close to the current footstep's position heading, the current inertial recursive heading has no directly relationship with the position heading between adjacent footsteps. Therefore, using the reference corridor heading to revise the inertial recursive heading is not suitable.

Height divergence is also a major problem in INS-based foot-mounted PDR system in multi-story positioning. The methods used in the literature mainly use the pitch angle [19] or the height change [20] of adjacent footsteps to determine whether a pedestrian is walking on the horizontal surfaces or stairs. Then using the height limitation method constrains the height divergence. As the pitch angle and height of the inertial recursion inherently have errors, directly using them to determine whether a pedestrian is walking on horizontal surfaces or stairs is prone to errors. Moreover, the method in the literatures mainly corrects the height error in the case of a plane, but does not correct the error in the case of stairs.

Based on the above analysis, in order to improve the robustness of the foot-mounted PDR system, in this paper, there are three contributions made as follows:

First, a novel stationary phase detection method is proposed which is based on foot motion periodicity rather than totally based on threshold comparison principle in the traditional method. In experiment, we found that the zero-speed state points always occur around the minimum value of stationary detector in each gait cycle. Moreover, under various motions, the magnitude of the zero-velocity detector T's value at the beginning and ending of each gait cycle is much greater than that within the gait cycle. Therefore, by setting a fuzzy suitably greatly magnitude threshold, the rough start and end times of each gait cycle can effectively be distinguished. Then, taking the minimum value of each gait cycle as the zero-speed state point, it can effectively detect the zero-speed points of each gait cycle under various pedestrian motions.

Second, based on the above analysis of HDE and iHDE methods' problem, an improved method has been proposed in this paper, which uses the reference heading to calculate the estimate position at the current footstep, then using the position error between the estimate position and the inertia recursive position restrains the heading divergence, which is more effective than the existing HDE and iHDE methods.

Third, for the height limitation, a more effective method has been proposed to determine the state of pedestrians by using the slope (height difference divided by stride length) between adjacent one/several footsteps. If pedestrian walking on the horizontal surfaces, keep the height always unchanged.

FIGURE 1. The IMU-based foot-mounted PDR system.

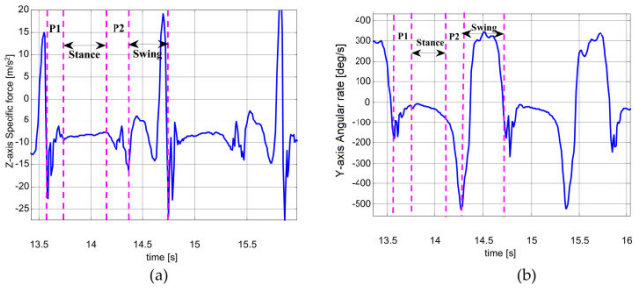

FIGURE 2. Pedestrian gait cycles: (a) two gait-cycle outputs of z-axis accelerometer; (b) two gait-cycle outputs of y-axis gyroscope.

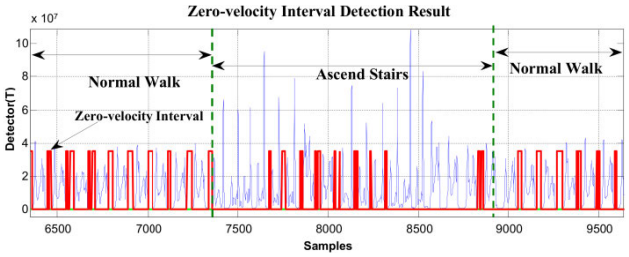

FIGURE 3. The zero-velocity interval detection result containing both normal walking and ascending stairs.

While walking on stairs, we propose using the slope of the stairs (usually 20 ∼ 45 degrees) to constrain the height divergence of the current footstep.

The layout of this paper is as follows: in Section II, the novel stationary phase detection method has been explained; In section III, the improved HDE algorithm proposed by this paper has been described and the detailed formula derivation has also been shown. In section IV, the novel height update algorithm based on the pedestrian adjacent footsteps' slope has been presented. In section V, the three proposed methods in this paper are analyzed in detail, and compared with the existing methods, the effectiveness of the proposed methods is proved. At last, in section VI, we conclude this paper's work and offer some future research suggestions.

II. THE NOVEL STATIONARY PHASE DETECTION ALGORITHM

The use of IMU sensors to obtain high precision of human motion positioning is challenging because it is largely affected by the drift of the IMU sensors. Fortunately, the human foot gait includes two stages: standing and swinging [21]. This can be used to estimate the impact of IMU drift. In the standing stage, human feet stand at the ground, therefore, their actual speed is close to zero. If the IMU's foot speed at this stage is different from zero, it must be due to an error caused by the IMU drift. Then, we can apply the ZUPT algorithm to reduce the drift of the IMU and improve the accuracy of the positioning. Therefore, the accuracy of the standing phase detection is crucial for achieving higher human foot positioning accuracy.

A. GAIT CHARACTERISTICS ANALYSIS

The pedestrian navigation shoe based on a self-contained sensor is shown in Figure 1, where all of the sensors are integrated in a structure to constitute an IMU, which includes a three-axis accelerometer and three-axis gyroscope. The IMU is fixed on the foot surface. When the pedestrian starts walking, the IMU constantly measures the acceleration and the angular rate of foot motion [22].

The pedestrian gait cycle shown in Figure 2 is obtained using the navigation shoe to collect the inertial parameters of a pedestrian's foot motion during movement. Figure 2a stands for the z-axis accelerometer output, which denotes the most varied acceleration, and Figure 2b represents the y-axis gyroscope output, which is the dominant rotation axis during movement. Figure 2a,b have two pedestrian gait cycles of the same period. The first gait cycle is divided into four stages, which are P1, stance, P2, and swing. P1 stage stands for the process from the heel striking the ground to the front sole striking the ground. Stance stage is the front sole contacting the ground completely, during which the sensors' outputs are approximately constant. This period is also called the zero-velocity interval, which is the most important stage to reduce the drift of the IMU by using ZUPT method. After the stance stage, the lift foot stage (P2) starts from the heel of the foot lifting off the ground to the moment of the toe. After that, the foot lifts off the ground, the leg begins to swing, and the body moves forward, which is the swing stage. After the swing phase, the heel of the foot strikes the ground again, which marks the beginning of another gait cycle.

B. ANALYSIS OF THE EXISTING STATIONARY PHASE DETECTION METHOD

The majority of zero-velocity detection methods employ comparisons between thresholds and the magnitude of acceleration, moving variance of acceleration, magnitude of angular rate, or their combinations. The primary limitation of these methods is that the variations in acceleration and angular rate differ greatly under various movement modes, such as walking, running, stair-climbing, etc. Thus, it is difficult to find a threshold function or threshold value that is widely applicable. We demonstrate this in Figures 3 and 4.

The general likelihood ratio test (GLRT) method [7], which is the most commonly used method to detect the zero-velocity interval, is employed in Figures 3 and 4. It uses the output of both the accelerometers and gyroscopes during the pedestrian movement. Therefore, its zero-velocity interval

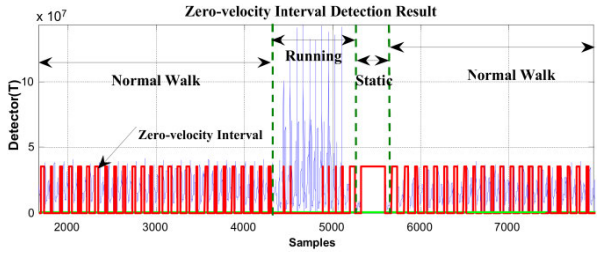

FIGURE 4. The zero-velocity interval detection result containing both normal walking and running.

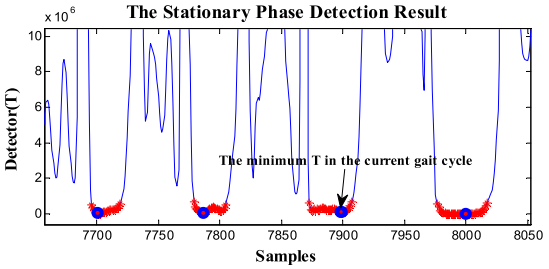

FIGURE 5. The stationary phase detection result during foot movement (The red "∗" points are the detection results of GLRT method and the blue " ∘ " points are the minimum value of detector T in each gait cycle.).

detection result is better than other algorithms based on threshold comparison. By using this method, the constructed zero-velocity interval detector T can be denoted as follows:

$$T\left(z_n^a, z_n^w\right) = \frac{1}{W}\sum_{k=n}^{n+W-1}\left(\frac{1}{\sigma_a^2}\left\|y_k^a - g\frac{\bar{y}_n^a}{\left\|\bar{y}_n^a\right\|}\right\|^2 + \frac{1}{\sigma_w^2}\left\|y_k^w\right\|^2\right) \tag{1}$$

where y_k^a and y_k^w denote the specific force vector and angular rate vector, respectively. σ_a^2 and σ_w^2 denote the variance of the measurement noise of the accelerometers and gyroscopes, respectively. Furthermore, $\|a\|^2 = a^T a$, where $(\cdot)^T$ denotes the transpose operator. Moreover, $\bar{y}_n^a$ denotes the sample mean, i.e.,

$$\bar{y}_n^a = \frac{1}{W}\sum_{k=n}^{n+W-1} y_k^a \tag{2}$$

The principle of the GLRT method is that, by comparing the magnitude of detector T in Equation (1) with a threshold, it can determine whether the current moment is in the zero-velocity interval.

In Figures 3 and 4, the red line represents the stationary state and moving state, where large values indicate the zero-velocity points and small values indicate the moving state. Figure 3 shows the zero-velocity interval detection result of movement containing both normal walking and ascending stairs. As we can see, although the threshold of the GLRT detector performs well during normal walking, when the pedestrian ascends stairs, the threshold fails to detect the zero-velocity interval during this period (near Sample 7500 and Sample 8500 in Figure 3). Figure 4 shows the zero-velocity interval detection result of movement containing both normal walking and running. Similarly, the threshold of GLRT detector performs well during normal walking, while it fails during the running period (between Sample 4000 and Sample 5000 in Figure 4).

In addition, in the literature [23], [24], some adaptive threshold zero-velocity interval detection algorithms were proposed. The basic detection principle is same as the GLRT method, which mainly involves constructing the zero-speed interval detector and comparing the detector with the threshold value to determine whether the current moment is in the zero-velocity interval. The mainly difference is that these algorithms can adaptively change the detection threshold using the established approximation relationship between the motion characteristics and the threshold. However, the effect of this method is not obvious for the random motion generated during actual movement. At the same time, the adaptive model algorithm is not universally applicable to different people.

C. THE PROPOSED NOVEL STATIONARY PHASE DETECTION METHOD

In section A, we have pointed out the periodicity of pedestrian movement. By detecting the periodic zero speed interval during pedestrian movement, the ZUPT algorithm can effectively reduce the drift of the IMU and improve the positioning accuracy of the navigation shoes. However, as shown in section B, the primary limitation of the existing stationary detection method is the variations in acceleration and angular rate differ greatly under different motion modes, such as walking, running, stair climbing, etc. Thus, it is difficult to find a threshold function or threshold value that is widely applicable.

By analyzing the result of Figure 3 and Figure 4, it is found that the zero-speed state points in each gait cycle always occur around the minimum value of the detector T in the period.

Just as shown in Figure 5, the red "∗ " points are the detection results of GLRT method, and the blue " ∘" points are the minimum detector point in each gait cycle. The red "∗" points always occurs around the blue "∘" points. And, it is a universally applicable rule to all kinds of movements including walking, running, stair climbing, etc. Therefore, if the zero-speed state points in each gait cycle want to be detected accurately under various motion states, the key is to find the minimum value of the detector T in this period, and then select some neighboring points as the zero-speed points simultaneously. Same as the principle of GPS/INS [15] combined navigation system, for the ZUPT-aided PDR system, there is only need to periodically correct the inertial recursive result, then, the divergence of the position result can be constrained. There is no necessary to detect all the zero-speed state points in one gait cycle. In other words, in each gait cycle, only using the minimum value of the detector T and some points around it as zero-speed points are sufficient to constrain the divergence of the inertial recursive position result.

Based on the above analysis, the proposed novel stationary phase detection method is based on the rule of finding

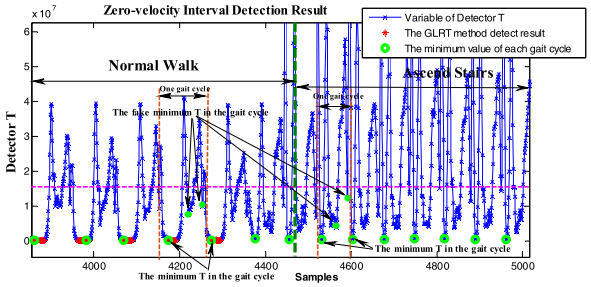

FIGURE 6. The stationary phase detection result during foot movement containing both normal walking and ascending stairs. (The red "∗" points are the detection results of GLRT method and the green " ∘" points are the minimum value of detector T in each gait cycle.).

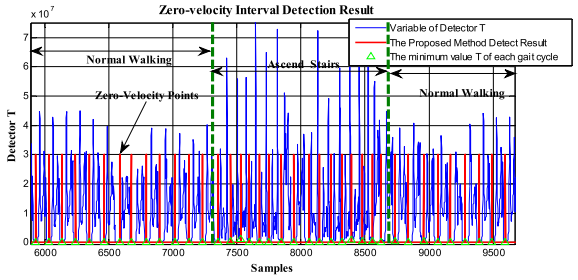

FIGURE 7. The zero-velocity point detection result of movement containing both normal walking and ascending stairs using the proposed method.

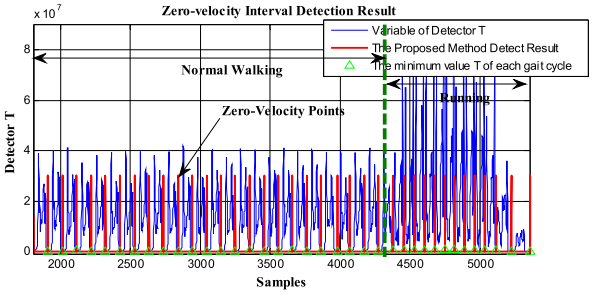

FIGURE 8. The zero-velocity point detection result of movement containing both normal walking and running using the proposed method..

the minimum value detector of each gait cycle. Firstly, as equation (1) is a commonly useful method to construct the zero-velocity interval detector T. So, it is still used to construct zero-velocity interval detector in our method. Secondly, although the variations of stationary phase detector T differ greatly under different motion modes (such as walking, running, stair climbing, etc.), the detector T still has a wide range of common variable fluctuation intervals under different motion modes (see Figure 6). It is also a universally applicable rule to all kinds of movements including walking, running, stair climbing, etc. Such as, in Figure 6, the pedestrian movement contains both normal walking and the ascending stairs. The variation of detector T(see variable on the vertical axis) still has wide range common interval under the two motion modes. In order to correctly find the minimum value of detector T in each gait cycle under various pedestrian movement, a large fuzzy threshold (indicated by the dashed magenta line in Figure 6) has been set to find the interval where the minimum T exists. And the value of the dashed magenta line only needs to be selected in the common variable interval of different motion modes. Using the threshold line, the rough start and end times of each interval that contained minimum T can be effectively distinguished. In Figure 6, taking one gait cycle (between two brown dashed lines near Sample 4200) under normal walking as an example, three intervals that are smaller than the set threshold line have been found. And in each interval, there is one minimum point, that is, there are three minimum points in this gait cycle. But only the minimum point in this whole gait cycle can be used as the zero-speed state point, that is, only the first minimum point is the real minimum T of the gait cycle and the other two are fake minimum T. As the magnitude of the real and the fake minimum T's values obviously is not in the same level, thus, each time after finding the minimum detector in each interval, we still need to compare them each other to find the smallest T in this gait cycle. Meanwhile, to ensure correctness, also compared it with the previous zero-speed state point T. If the values of them are in the same magnitude, then it can be confirmed as true zero-speed point of current gait cycle, otherwise it is fake zero-speed point. This method is also applicable to running and other motions.

In the switching phase of different movements, the minimum T's magnitude of zero-speed state point in the gait cycle will change (see Figure 6, switch from normal walking to ascend stairs). However, the minimum T's magnitude of zero-speed point under different movements is relatively close, while the minimum T's magnitude of fake zero-speed status points is always much greater than the T's magnitude of zero-speed point under different movements.

In addition, a static detection algorithm is added to the proposed method to detect the pause or standstill state during the gait cycle. If the standstill or pause state is detected, the previous navigation state (position, velocity, and attitude) is directly used as the current navigation state to constrain the divergence of the inertial recursive results.

In order to verify the effectiveness of the proposed method, the data in Figure 3 and Figure 4 are reprocessed by the proposed method, and the results are shown in Figure 7 and Figure 8. Compared with the case of missing detection near Sample 7500 and Sample 8500 after switching from the normal walking to ascending stairs in Figure 3, it can be seen from Figure 7 that the missed detection condition is effectively improved. At the same time, compared to the case of missing detection between Sample 4000 and Sample 5000 after switching from normal walking to running phase in Figure 4, the overall zero-speed point detection has been well improved in Figure 8.

The proposed method to detect the zero-speed points under various movements is described in Algorithm 1.

The coordinates mentioned below in this paper are all in the geographic coordinate system or Gauss plane coordinate system.

Algorithm 1 The Novel Stationary Phase Detection Algorithm

Initiate: at time $t \leftarrow 0$

$Threshold_0$: a large fuzzy threshold used to find the interval where the minimum T exists in each gait cycle under various pedestrian movements. In our experiment, $Threshold_0$ is $0.5e^{7} \sim 2e^{7}$ when using the Xsens Mtw IMU device the paper used.

Input: T: The stationary phase detector constructed by using Equation (1), which uses the output of both accelerometers and gyroscopes of foot motion.

Output: *zupt*: The detection result of zero-speed points during dynamic gait cycles.

Step 1: Static detection

Use the static detection algorithm to determine whether the pedestrian is in a static state. If the pedestrian in a static state, directly use the previous navigation state (position, velocity, and attitude) as the current navigation state to constrain the divergence of the inertial recursive results. If in a dynamic state, execute Step 2.

Step 2: Zero-speed point detection

Use the large fuzzy threshold to find the interval where the minimum T exists in each gait cycle. Then, compare it with previous several minimum T to find the smallest T in current gait cycle. For insurance, also compare it with the previous zero-speed point T. If the values of them are in the same magnitude, it can be confirmed as the true zero-speed point, otherwise it is fake zero-speed point. If there is no zero-speed point T before, the current minimum T should compare with the following several minimum T, then the smallest T is selected as the zero-speed point.

Step 3: Repeat Step 1 and Step 2

Repeat Step 1 and Step 2 to continue detecting zero-speed points of each gait cycle until the pedestrian ends the movement.

III. THE IMPROVED HDE ALGORITHM

HDE method is an effectively approach to mitigate the heading error, where the known orthogonal indoor corridors' headings are used as the reference headings. The HDE and improved HDE (iHDE) methods mentioned in the existing literatures use the position heading between adjacent footsteps to determine whether pedestrian walks straight along the indoor corridor (the domain directions), and then use the heading error between the position heading and the closest reference corridor heading to correct the inertial recursive heading at the current footstep. However, the reference corridor heading is close to the position heading not the current inertial recursive heading which has no directly relationship with the position heading. Therefore, an improved method has been proposed in this paper, which uses the reference heading to calculate the estimate position at the current footstep, then uses the position error between the estimate position and the inertia recursive position to restrain the heading divergence.

A. HDE AND IHDE METHODS ANALYSIS

According to Abdulrahim [13] and Jimenez. A R's research [18], the process of HDE and iHDE methods consists of six steps, which are as follows:

1) Stride Heading ($\theta_S(k)$): Calculate the position heading using the plane position coordinate difference between adjacent footsteps when pedestrian moving:

$$\theta_S(k) = \arctan(\frac{y_k - y_{k-1}}{x_k - x_{k-1}}) \tag{3}$$

Here, k is the index of the k-th footstep. This stride heading is based on the difference in position caused by adjacent footsteps, and therefore it consists of not only the true inertial heading plus drift, but also other unmodelled errors from inertial navigation [13].

2) Stride Length ($SL(k)$): Calculate the stride length between adjacent footsteps when pedestrian moving:

$$SL(k) = \sqrt{(y_k - y_{k-1})^2 + (x_k - x_{k-1})^2} \tag{4}$$

Which will be later used to reject HDE corrections when walking with short stride. A threshold for the SL of 0.8m ($\mathrm{Th}_{SL} = 0.8\mathrm{m}$) is used.

3) Straight Line Path ($SLP(k)$): At least three user strides with similar orientation in order to classify a trajectory as straight. We compute a binary Straight-Line Path (SLP) parameter as:

$$SLP(k) = \begin{cases} 1 & \max(|\theta_S(j) - mean(\theta_S(j))|) < Th_\theta \\ & for\ \mathrm{j} = k : \mathrm{k} - 3 \\ 0 & Otherwise \end{cases} \tag{5}$$

Here, Th_θ is an angle threshold, and $Th_\theta = 15$ degrees are used in our method. SLP is used to deactivate the perturbing HDE corrections at curved paths.

4) The Indoor Major Direction (MD): Most of indoor corridors are in 4 or 8 major directions (called as dominant directions) and the difference of the major directions is usually 45° or 90°. The indoor major directions denote as follows:

$$\theta_{R_i} \quad \text{and i} = 1, 2, \cdots, 4 \quad or\ \mathrm{i} = 1, 2, \cdots, 8 \tag{6}$$

Here, θ_{R_i} denotes the indoor major directions and i indicates the number of the directions.

5) The heading Error: According Step 3), if pedestrians are walking straight ($SLP(k) = 1$) and the stride heading close to the dominant heading, the heading difference $\delta\theta$ (heading error) between the user's stride heading θ_S and the closest dominant directions of the building θ_R can be got:

$$\delta\theta(k) = \theta_S(k) - \theta_R \tag{7}$$

Here, $\delta\theta(k)$ is the heading error of k-th footstep.

6) Kalman Filter with the Heading Update

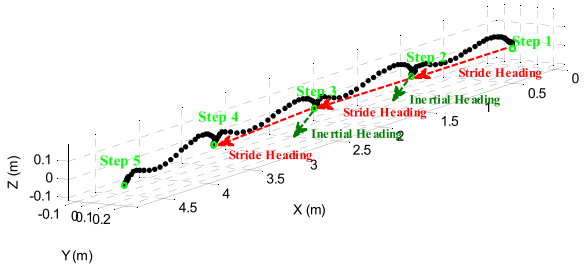

FIGURE 9. The real pedestrian indoor trajectory (walking straight).

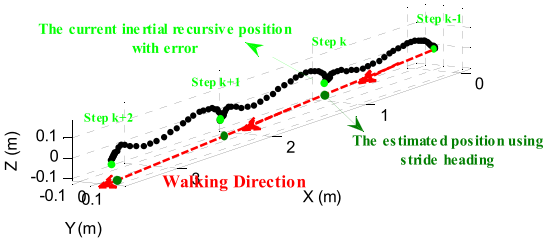

FIGURE 10. Revise the current step's inertial recursive position with the position calculated from the stride heading.

The state vector is as follows:

$$\mathrm{X} = (\,\delta\mathrm{p} \quad \delta\mathrm{v} \quad \delta\psi \quad \delta\mathrm{w} \quad \delta\mathrm{a}\,)^T \tag{8}$$

Here, δp, δv, $\delta\psi$, δw and δa represent the estimated INS errors of position, velocity, attitude (roll, pitch and yaw), angular rate, and acceleration, respectively.

The measurement vector is the stride heading error $\delta\theta(k)$ which got from Step 5). Then, using $\delta\theta(k)$ as the INS's inertial recursive heading error to estimate INS's state vector. Hence, the measurement matrix H is as follows:

$$\mathrm{H} = (\,0_{1\times3} \quad 0_{1\times3} \quad [\,0 \quad -\sin\varphi \quad 1\,] \quad 0_{1\times3} \quad 0_{1\times3}\,) \tag{9}$$

Here, Abdulrahim [13] believes that the stride heading error is related to the inertial heading errors, therefore, in measurement matrix H, simply using $-\sin\varphi$ and 1 represent their relationship.

However, in HDE and iHDE methods, the stride heading is the heading between adjacent footsteps which has no directly relationship with the current inertial heading. As shown in Figure 9, the stride heading is not same to the inertial heading of current footstep. Therefore, the stride heading error $\delta\theta(k)$ has no directly relationship with the current step's inertial recursive heading errors. Thus, using the stride heading error as the inertial recursive heading error to estimate INS's state vector is not suitable.

B. THE IMPROVED HDE ALGORITHM

Based on above analysis, an improved method has been proposed in this paper, and the major improvements are in Step 5) and Step 6).

In Step 5), The closest indoor major heading θ_R can be found based on the stride heading. A threshold for the heading difference of $\delta\theta(k) = 15$ degrees is used in our method. If the absolute difference between $\theta_S(k)$ and one of θ_R is less than 15 degrees, the θ_R is considered as the closest indoor major heading of current footstep. As the stride heading has no directly relationship with the current inertial heading, therefore, we use the major heading θ_R and the position of the previous footstep to calculate the current footstep's position, then use it to correct the current inertial recursive position. The principle of proposed method is as shown in Figure 10, at step k, the current inertial recursive position with error is indicated by the bright green dot, while the estimated step k's position calculated by the stride heading and the position of step k-1 is indicated by the nearest dark green dot.

As pedestrian is walking straight, the dark green dot is closer to the actual position of the pedestrian. Thus, using dark green dot's position can revise the current step's inertial recursive position effectively.

The derivation process of calculating the step k's plane position by using the major heading θ_R and the position of the step k-1 is as follows:

$$\begin{cases} \tan\theta_R = \dfrac{\hat{y}_k - y_{k-1}}{\hat{x}_k - x_{k-1}} \\ (\hat{y}_k - y_{k-1})^2 + (\hat{x}_k - x_{k-1})^2 = SL^2\,(k) \end{cases}$$

$$\Rightarrow \begin{cases} (\hat{y}_k - y_{k-1}) = \tan\theta_R\,(\hat{x}_k - x_{k-1}) \\ (\hat{y}_k - y_{k-1})^2 + (\hat{x}_k - x_{k-1})^2 = SL^2\,(k) \end{cases} \tag{10}$$

Here, θ_R is the closest indoor major heading. (x_{k-1}, y_{k-1}) is the inertial recursive position of step $k-1$. $(\hat{x}_k, \hat{y}_k)$ is step k's estimated coordinates which will be calculated. $SL\,(k)$ is the stride length between step k and step $k-1$, which can be calculated by equation (4) using the inertial recursive position of step k and step $k-1$.

Let:

$$\begin{cases} \hat{y}_k - y_{k-1} = \mathrm{Y} \\ \hat{x}_k - x_{k-1} = X \end{cases} \tag{11}$$

Substituting (11) into (10), then:

$$\begin{cases} Y = \tan\theta_R X \\ Y^2 + X^2 = SL^2\,(k) \end{cases} \tag{12}$$

Then:

$$\begin{cases} X^2\left(1 + \tan^2\theta_R\right) = SL^2\,(k) \\ Y^2 + \dfrac{1}{\tan^2\theta_R} Y^2 = SL^2\,(k) \end{cases} \tag{13}$$

Therefore, using the step $k-1$'s coordinate x_{k-1}, the current step k's coordinate $\hat{x}_k$ can be got:

$$\begin{aligned} X^2\left(1 + \tan^2\theta_R\right) &= SL^2\,(k) \\ X &= \pm\frac{SL\,(k)}{\sqrt{1 + \tan^2\theta_R}} \\ \hat{x}_k - x_{k-1} &= \pm\frac{SL\,(k)}{\sqrt{1 + \tan^2\theta_R}} \\ \hat{x}_k &= x_{k-1} \pm \frac{SL\,(k)}{\sqrt{1 + \tan^2\theta_R}} \end{aligned} \tag{14}$$

Similarly, the current step k's coordinate $\hat{y}_k$ can be got:

$$\begin{aligned} Y^2 + \frac{1}{\tan^2\theta_R} Y^2 &= SL^2(k) \\ \left(1 + \frac{1}{\tan^2\theta_R}\right) Y^2 &= SL^2(k) \\ Y &= \pm \frac{\tan\theta_R}{\sqrt{1+\tan^2\theta_R}} SL(k) \\ \hat{y}_k - y_{k-1} &= \pm \frac{\tan\theta_R}{\sqrt{1+\tan^2\theta_R}} SL(k) \\ \hat{y}_k &= y_{k-1} \pm \frac{\tan\theta_R}{\sqrt{1+\tan^2\theta_R}} SL(k) \end{aligned} \tag{15}$$

Therefore, the step k's estimated plane position calculated from the closest major heading θ_R and the position of the step k-1 is as follows:

$$\begin{cases} \hat{x}_k = x_{k-1} \pm \dfrac{SL(k)}{\sqrt{1+\tan^2\theta_R}} \\ \hat{y}_k = y_{k-1} \pm \dfrac{\tan\theta_R}{\sqrt{1+\tan^2\theta_R}} SL(k) \end{cases} \tag{16}$$

Here, the sign $\pm$ in (16) can be decided by the sign of the difference of the inertial recursive position of step $k-1$ and step k.

Then, using the step k's estimated plane position $(\hat{x}_k, \hat{y}_k)$ and the EKF framework revise the current step's inertial recursive errors.

Therefore, in step 6), the main purpose is to perform the EKF update based on the position error. The state vector is same as before:

$$\mathrm{X} = (\,\delta\mathrm{p} \quad \delta\mathrm{v} \quad \delta\psi \quad \delta\mathrm{w} \quad \delta\mathrm{a}\,)^T \tag{17}$$

The measurement vector is the current step's position error. And, the measurement matrix H is as follows:

$$\mathrm{H} = \left(\begin{bmatrix} 1 & & \\ & 1 & \\ & & 0 \end{bmatrix} 0_{3\times3}\ 0_{3\times3}\ 0_{3\times3}\ 0_{3\times3} \right) \tag{18}$$

Here, as the proposed improved HDE method is mainly for the correction of the plane position, not for the height. Thus, in H, the position correlation matrix is $diag(1, 1, 0)$.

The proposed improved HDE algorithm is described in Algorithm 2.

Algorithm 2 The Improved HDE Algorithm

Initiate: at time $t \leftarrow 0$

The Indoor Major Heading: Most of indoor corridors are in 4 or 8 major directions (called as dominant directions), which used as the reference heading in improved HDE method.

$$\theta_{R_i} \text{ and i} = 1, 2, \cdots, 4 \; or \text{i} = 1, 2, \cdots, 8$$

Input: *Stride Heading*: $\theta_S(k)$;
Stride Length: $SL(k)$;
Straight Line Path: $SLP(k)$;
Indoor Major Heading: θ_R;

Output: E*stimated state error vector*:

$$\mathrm{X} = (\,\delta\mathrm{p}\ \delta\mathrm{v}\ \delta\psi\ \delta\mathrm{w}\ \delta\mathrm{a}\,)^T$$

Using the estimated state error vector, the divergence of inertial recursive error can be restrained.

Step 1: Determine if $SL(k) > 0.8m$ and $SLP(k) = 1$.
If the conditions are met, the pedestrian is moving straight. Then proceed to Step 2.

Step 2: Determine the closest major heading θ_R
If the difference between $\theta_S(k)$ and one of θ_R is less than 15 degrees, the θ_R is considered as the closest indoor major heading of current footstep.

Step 3: Calculate the footstep k's plane position $(\hat{x}_k, \hat{y}_k)$ by using the major heading θ_R and the position of the footstep $k-1$.
The detailed process is as described before.

Step 4: Estimate the state error vector
Using the estimated plane position $(\hat{x}_k, \hat{y}_k)$ and the EKF framework estimate the state error vector. Then, using the state error vector revises the current footstep's position, speed and attitude (roll, pitch and yaw).

Step 5: Repeat Step 1- Step 4
Repeat Step 1-4 until the pedestrian ends the movement.

IV. THE HEIGHT UPDATE ALGORITHM

Height divergence is a major problem in INS-based foot-mounted PDR system in multi-story positioning. The methods used in the literature mainly use the pitch angle or the height change of adjacent footsteps to determine whether a pedestrian is walking on a plane or a staircase. Then using the height limitation method constrains the height divergence. As the pitch angle and height of the inertial recursion inherently have errors, directly using them to determine whether a pedestrian is walking on horizontal surfaces or stairs is prone to errors. In this section, a more effective method has been proposed to determine the state of pedestrians by using the slope (height difference divided by stride length) between adjacent one or several footsteps, as shown in Figure 11. If pedestrian walking on a plane, the slope of the current stride is approximately zero degree, if that, keep the height always unchanged. While walking on a staircase, we proposed to use the actual slope of the stairs (usually $20 \sim 45$ degrees) to calculate the height change of the current stride, which can be used to constrain the height divergence of the current stride.

First, the proposed method needs to calculate some judgment detectors. The detectors are as follows:

1) Stride Length ($SL(k)$): The calculation equation is same to equation (4). Also, a threshold for the $SL(k)$ of 0.8m ($\mathrm{Th}_{SL} = 0.8\mathrm{m}$) is used.
2) Slope Angle ($\theta_{\mathrm{Slope}}(k)$): Calculate the slope angle between adjacent one/several footsteps. At here,

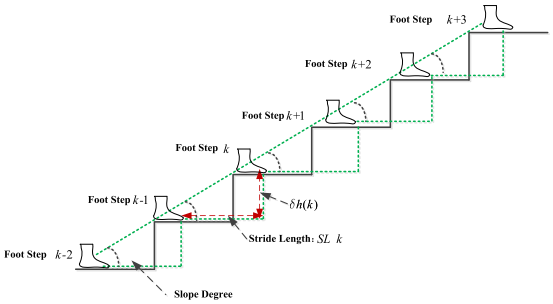

FIGURE 11. The slope definition of adjacent footsteps.

the slope angle is calculated by using the height difference and the stride length between adjacent one footstep. The detailed calculation equation is as follows:

$$\theta_{\text{Slope}}(k) = \arctan(\frac{h_k - h_{k-1}}{SL(k)}) \tag{19}$$

Here, k is the index of the k-th footstep. h_k and h_{k-1} is the height of footstep k and footstep k-1, respectively. $SL\ (k)$ is the stride length between footstep k and footstep $k-1$.

3) Same Slope Path ($SSP(k)$): At least three user strides with similar slope. We compute a binary Same-Slope Path (SSP) parameter as:

$$SSP\ (k) = \begin{cases} 1 & \max(\left|\theta_{Slope}(j) - mean(\theta_{Slope}(j))\right|) < Th_{\theta\_Slope} \\ & for \mathrm{j} = k : \mathrm{k} - 3 \\ 0 & Otherwise \end{cases} \tag{20}$$

Here, Th_{θ_Slope} is an angle threshold, and $Th_{\theta\_\text{Slope}} = 10$ degree is used in our method. SSP is used to deactivate the perturbing height corrections at non-planar and non-staircase.

4) The Height Error: If the current footstep k meets the requirement of Step 3), the pedestrian is walking on the plane or stairs. Then, if the current slope angle $\theta_{\text{Slope}}(k)$ is close to zero, the current footstep k is considered to be walking on a plane, which means the current footstep k's height should same to the footstep k-1. Thus, the height error of current footstep k is:

$$\delta h(k) = h_{k-1} - h_k \tag{21}$$

While the current slope angle $\theta_{\text{Slope}}(k)$ is over 20 degrees, the current footstep k is considered to be walking on staircases (see Figure 11). If the actual slope of the stair is 30 degrees, the height change from footstep $k-1$ to k can be calculated as follows:

$$\Delta h(k) = SL(k) * \tan(30 * (\text{pi}/180)) \tag{22}$$

Here, $SL(k)$ is the stride length between footstep k and $k-1$, as shown in Figure 11.

TABLE 1. The specification of the MTw inertial measurement unit (IMU) device. ACC—accelerometer; GYR—gyroscope; MAG—magnetometer; BAR—barometer.

Specification	Acc	Gyro	Mag	Bar
Sensor type	Analog	Analog	Digital	Digital
Full scale	$\pm 160 m/s^2$	$\pm 1200 \deg/s$	$\pm 1.5 Gauss$	300-1100hPa
Linearity	0.2%	0.1%	0.2%	0.05%
Bias stability	-	$20 \deg/hour$	-	$100\ Pa/year$
Noise	$0.003 m/s^2/\sqrt{Hz}$	$0.05 \deg/s/\sqrt{Hz}$	$0.15 mGauss/\sqrt{Hz}$	$0.85\ Pa/\sqrt{Hz}$

Therefore, if the current footstep k is considered to be walking on the stairs, the height error is:

$$\delta h(k) = h_{k-1} \pm \Delta h(k) - h_k \tag{23}$$

Here, the sign $\pm$ in (23) can be decided by the sign of the inertial recursive height difference between footstep $k-1$ and k.

5) Kalman Filter with the Height Update The state vector is as follows:

$$\mathrm{X} = (\ \delta \mathrm{p} \quad \delta \mathrm{v} \quad \delta\psi \quad \delta \mathrm{w} \quad \delta \mathrm{a}\ )^T \tag{24}$$

Here, δp, δv, $\delta\psi$, δw and δa represent the estimated INS errors of position, velocity, attitude, angular rate, and acceleration, respectively.

The measurement vector is the height error $\delta h(k)$ which got from Step 4). Hence, the measurement matrix H is as follows:

$$\mathrm{H} = \left(\begin{bmatrix} 0 & & \\ & 0 & \\ & & 1 \end{bmatrix} \quad 0_{3\times3} \quad 0_{3\times3} \quad 0_{3\times3} \quad 0_{3\times3} \right) \tag{25}$$

The proposed height update algorithm is described in Algorithm 3.

V. EXPERIMENTAL EVALUATION

In this section, we present the evaluation result of the heading and position of the foot-mounted PDR system using the proposed algorithms in a realistic test environment.

A. HARDWARE DESCRIPTION

The MTw IMU device from Xsens was used in the evaluation experiment. The IMU included three orthogonally oriented accelerometers, gyroscopes, magnetometers, and one barometer. The data output frequency of MTw was 100 Hz. In the experiment, the IMU device was fixed on the foot to collect pedestrian movement data (see Figure 1). The specification of the MTw device is shown in Table 1.

B. THE EXPERIMENT ROUTE LINE

1) TEST ROUTE 1

Figure 12 shows the test route in the building, where C1 and C2 are the spaces beside every floor's elevator (4.8 m × 7.2 m). S1 and S2 are the stairs between the floors. The slope angle of S1 and S2 is 30 degrees. Point A and Point F represent one side of the corridors, and they coincide on the projection plane, and the same goes for points B and E, Point C and Point D, Point H and Point G.

Algorithm 3 The Height Update Algorithm

Initiate: at time $t \leftarrow 0$

The actual slope of the staircase: The slope θ_{Slope} of indoor stairs is usually fixed, which between 20 to 45 degrees. The slope can be used to help the height limitation in the proposed height update algorithm.

Input: *Stride Length*: $SL(k)$;
Slope Angle: $\theta_{Slope}(k)$;
Same Slope Path: $SSP(k)$;
Actual slope of the indoor stairs: θ_{Slope};
If it is possible, obtain the actual slope θ_{Slope} of the indoor stairs in advance. If not, as the slope of the stairs is usually 20 ∼45 degrees, the average slope 30 degrees can be used to limit the height divergency.

Output: E*stimated state error vector*:

$$\mathrm{X} = (\,\delta \mathrm{p}\ \delta \mathrm{v}\ \delta\psi\ \delta \mathrm{w}\ \delta \mathrm{a}\,)^T$$

In order to unify with the state vector in algorithm 2, the state vector here is same as algorithm 2. Here, it is mainly used to estimate the height error.

Step 1: Determine if $SL(k) > 0.8m$ and $SSP(k) = 1$.

If the conditions are met, the pedestrian is moving on a plane or stairs. Then proceed to Step 2.

Step 2: Determine pedestrian walking on the plane or stairs.

If the current slope angle $\theta_{Slope}(k)$ is close to zero, the current footstep k is considered to be walking on the plane. While the current slope angle $\theta_{Slope}(k)$ is over 20 degrees, the current footstep k is considered to be walking on staircase.

Step 3: Calculate current footstep k's height error $\delta h(k)$

If pedestrian moves on the plane, the height error is shown in equation (21), while pedestrian moves on the stairs, using equation (23) calculates height error of footstep k.

Step 4: Estimate the state error vector

Using the footstep k's height error $\delta h(k)$ and the EKF framework estimate the state error vector X. Then, using the state error vector X revises the inertial recursive error.

Step 5: Repeat Step 1-Step 4

Repeat Step 1-4 until the pedestrian ends the movement.

2) TEST ROUTE 2

Test route 2 is shown in Figure 13, which is a ring road and the length is about 500m. The absolute heading between Point 8 and Point 1 has been measured in advance, which is $\theta_{R1} = 159.187$ degrees. Similarly, the absolute heading between Point 2 and Point 3, Point 4 and Point 5, Point 6 and Point 7 are $\theta_{R2} = 69.187$ degrees, $\theta_{R3} = -20.813$ degrees, and $\theta_{R4} = -110.813$ degrees, respectively. The experimental data collection process starts from the starting point, then walks counterclockwise, walks around the ring road for twice, and finally returns to the starting point.

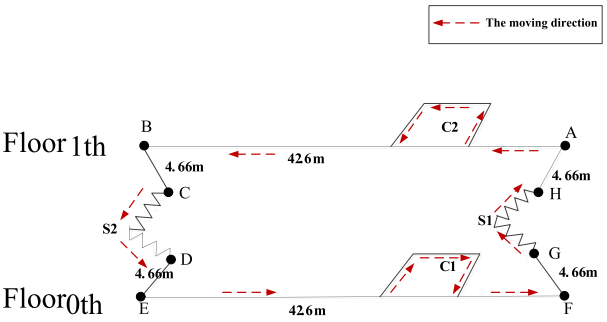

FIGURE 12. Test route 1.

FIGURE 13. Test route 2.

C. THE STATIONARY PHASE DETECTION EXPERIMENT

Since test route 1 including stairs, pedestrians could go up and down stairs and perform various types of movements in the corridor, effectively evaluating the effectiveness of the zero-speed interval detection algorithm proposed in this paper. Therefore, we used test route 1 to verify the zero-speed interval detection algorithm proposed in this paper. At the same time, as a comparison, the same test data was processed by the GLRT algorithm, and the obtained positioning trajectory was compared with the trajectory processed by the proposed algorithm.

The experimental data collection process is as follows: the pedestrian started movement from point A of Floor 1, walked along the corridor, went around in C2, then ran along the corridor for a while, after reached point B, went down the stairs from S2, and arrived at point E of Floor 0. On Floor 0, similarly to Floor 1, the pedestrian walked along the corridor, then ran for a while, then went around in C1, after reached point F, went upstairs through S1, and finally arrived at the starting point A of Floor1.

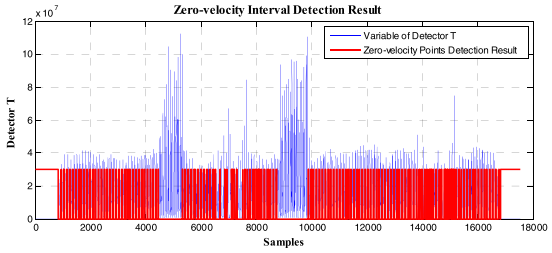

FIGURE 14. The zero-velocity interval detection result using the GLRT method.

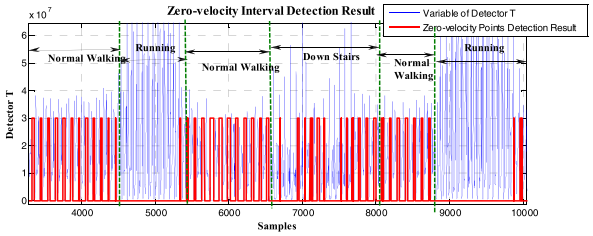

FIGURE 15. The zero-velocity interval detection result using the GLRT method.

1) TEST RESULT USING THE GLRT METHOD

Using the GLRT method to process the test data collected in test route 1, the overall zero-speed interval detection result is shown in Figure 14. In Figure 14, the horizontal axis represents the sampling points, and the vertical axis is the variable of detector T. The red line in the figure represents the stationary state and moving state, where large values indicate the stationary interval, while small values indicate the moving interval. As we can see, between Sample 4000 and Sample 5000, there has obviously missing detections. Similarly, there also has missing detections between Sample 8000 and Sample 10,000. In order to better observe the missing detections, the detection results from Sample 4000 to Sample 10,000 are enlarged and displayed in Figure 15.

In Figure 15, as we can see, the GLRT method performs well during normal walking, but when the pedestrian in the running state (around Sample 5000), it fails to detect the zero-velocity interval and have missing detections during this period. Similarly, after switching from walking to going downstairs state (around Sample 7000), there have obviously failed detections during this period.

Based on the zero-speed interval detected results shown in Figures 14 and 15, the pedestrian plane positioning trajectory is shown in Figure 16. The trajectory from C1/C2 to the side of point B/E should be a straight line (see Figure 12), and the trajectories of Floor 0 and Floor 1 should be basically coincident. However, in Figure 16, since the GLRT method obviously failed detections during the running state and going downstairs state, there is a serious shift in the pedestrian positioning trajectory.

2) TEST RESULT USING THE PROPOSED METHOD

In the experiment, using the proposed method to process the same test data collected in test route 1. As we can see,

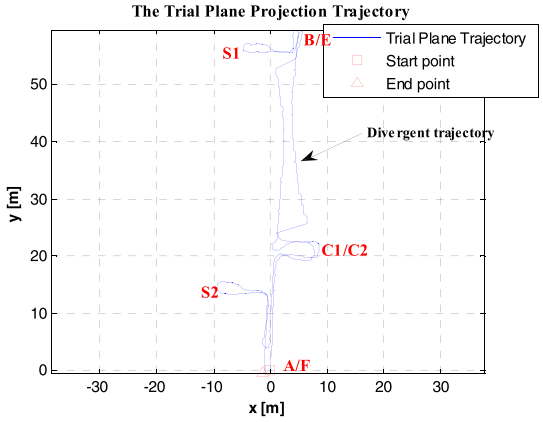

FIGURE 16. Pedestrian positioning trajectory based on the GLRT method.

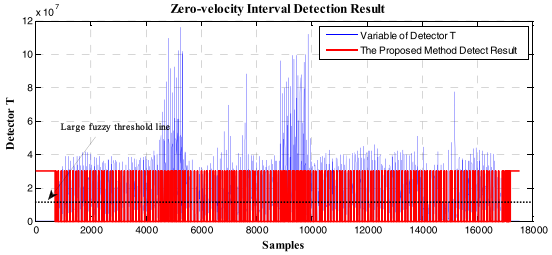

FIGURE 17. The zero-velocity interval detection result using the proposed method.

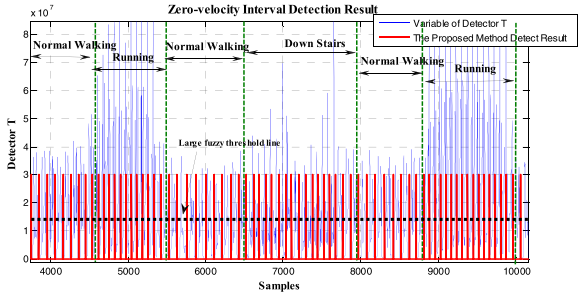

FIGURE 18. The zero-velocity interval detection result using the proposed method.

the detector T(see the vertical axis of Figure 17) has a wide range of common variable fluctuation intervals roughly between 1×10^7 and 2×10^7 under different motion modes (including normal walking, running, down stairs, etc.). Therefore, the large fuzzy threshold is chosen between 1×10^7 and 2×10^7 (the black dotted line in Figure 17). The overall zero-speed point detection results are shown in Figure 17. Compared to the missing detections in Figure 14, the proposed method effectively detected the zero-speed points of each gait cycle. The partial enlargement result of Figure 17 is also shown in Figure 18.

In Figures 17 and 18, the red line represents the stationary state and moving state, where large values indicate the stationary interval, and small values indicate the moving interval. Similarly, compared to the missing detections in Figure 15, the proposed method performed well

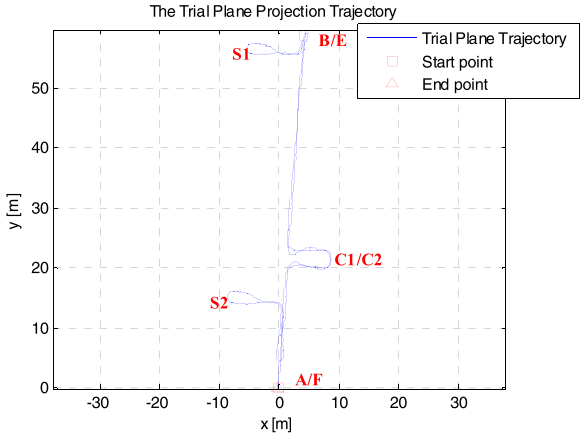

FIGURE 19. Pedestrian positioning trajectory processed using the proposed method.

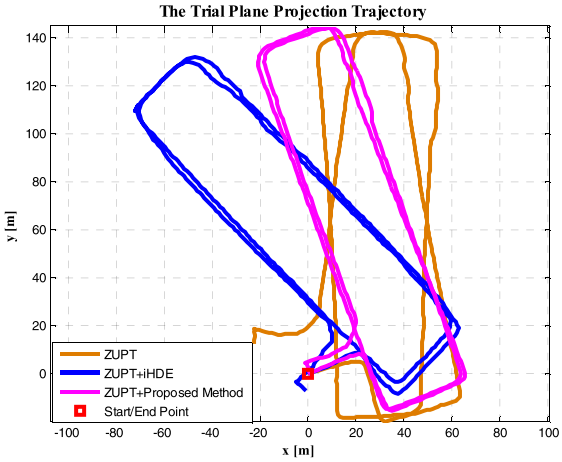

FIGURE 20. Pedestrian test plane projection trajectories after using three heading constraint algorithms. The brown line indicates only using ZUPT algorithm, the blue line indicates using ZUPT +iHDE (the method used in literatures), while the magenta line indicates using ZUPT + proposed heading constraint algorithm.

(see Figure 18) not only during normal walking, but also during the running state and going downstairs.

Based on the zero-speed interval detection results using the proposed method (as shown in Figures 17 and 18), the pedestrian plane positioning trajectory is shown in Figure 19. Compared to the offset and divergence of the trajectory in Figure 16, the positioning result in Figure 19 shows considerable improvement. The obtained trajectory is basically the same as the test route, and the trajectories of Floor 0 and Floor 1 are coincident.

D. THE IMPROVED HDE ALGORITHM EXPERIMENT

In test route 2, pedestrian starts walking from the start point, then walks counterclockwise around the ring road for twice, finally returns to the start point, with a total trajectory length of about 1000m. Therefore, it can be well used to verify the effectiveness of the heading calibration algorithm during pedestrian walking for long time and long distances. Here, the reference headings are the absolute heading between Point 8 and Point 1, Point 2 and Point 3, Point 4 and Point 5, Point 6 and Point 7, which are $\theta_{R1} = 159.187$ degrees, $\theta_{R2} = 69.187$ degrees, $\theta_{R3} = -20.813$ degrees, and $\theta_{R4} = -110.813$ degrees, respectively.

At the same time, as a comparison, the iHDE method proposed by Jimenez. A R in literature [17] also has been analyzed in this section. As mentioned in part A of section III, it mainly uses the position heading between adjacent footsteps to determine whether pedestrian walks straight along the indoor corridor (the domain directions), and then uses the closest reference corridor heading to correct the pedestrian inertia recursive heading at the current footstep. However, the reference corridor heading is close to the current footstep's position heading not the current inertial recursive heading which has no directly relationship with the position heading. Therefore, in the proposed method of this paper, it manly uses the reference heading to calculate the estimate position of current footstep, then uses the position error between the estimate position and the current inertia recursive position to restrain the heading divergence.

In Figure 20, the plane projection trajectories after using three heading constraint algorithms have been shown. The brown line indicates only using ZUPT algorithm, the blue line indicates using ZUPT + iHDE (the method used in literatures), while the magenta line indicates using ZUPT + proposed heading constraint algorithm. As we can see, when only using the ZUPT algorithm, the two loop trajectories that should be coincident have deviated severely, and the start and end points should have coincided, but they have not coincided. Because ZUPT algorithm mainly used to revise the velocity and has little effect on the heading correction of the trajectory. When using ZUPT + iHDE algorithm, the trajectory's heading can be revised, the two loop trajectories can overlap well, although the ending point of the trajectory has shifted and does not coincide with the starting point. But as we state before, the iHDE method mainly uses the position heading between adjacent footsteps to find the closest reference heading, then uses it to revise the pedestrian inertia recursive heading. Although the reference heading can constrain the inertial recursive heading, the trajectory heading cannot be restricted to the correct angle reasonably. This will be further analyzed in Figure 21. When using ZUPT+ proposed heading constraint algorithm, similarly, the two loop trajectories can be overlap well. Moreover, the starting and ending points of the trajectory can be overlapped well.

In Figure 21, the trajectory's position headings between adjacent footsteps have been shown after the trajectory processed by the three algorithms. The yellow line indicates only using ZUPT algorithm, the blue line indicates using ZUPT + iHDE, while the black line indicates using ZUPT + proposed heading constraint algorithm. The four reference headings are indicated by red dashed lines: R1, R2, R3, R4, which represent 159.187 degrees, 69.187 degrees, −20.813 degrees and −110.813 degrees, respectively. S5 and S9 denote the heading when pedestrian walks from Point 8 to Point 1. As we can see, the black line is very close to the R1 (the

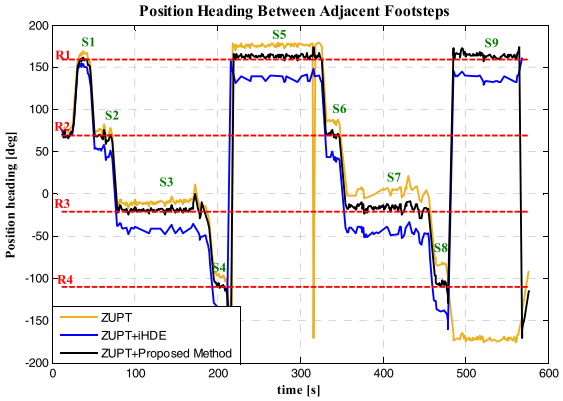

FIGURE 21. The trajectory's position heading between adjacent footsteps after using the three heading constraint methods. The yellow line indicates only using ZUPT algorithm, the blue line indicates using ZUPT +iHDE (the method used in literatures), while the black line indicates using ZUPT + proposed heading constraint algorithm. The red dotted lines are the four reference heading lines (R1, R2, R3, R4), respectively.

reference heading: 159.187 degrees) after using ZUPT + proposed method, while the yellow line (using ZUPT + iHDE method) and the blue line (only using ZUPT method) have already deviated from R1. Similarly, S3 and S7 denote the heading when pedestrian walks from Point 4 to Point 5. The black line is also very close to the R3 (the reference heading: −20.813 degrees), while the yellow line and the blue line still have deviated from R3. The same is true for S1, S2, S4, S6 and S8, the black lines using the proposed method are closer to the reference heading, while the yellow line and the blue line are off the reference line to some extent. Therefore, although from Figure 20, ZUPT + iHDE method has a good effect on the constraint of trajectory's heading and the trajectory overlaps well, from Figure 21 we know this method cannot constrain the trajectory's heading to the reference heading correctly. However, when using ZUPT + proposed heading constraint algorithm, the trajectory's heading can be correctly constrained from both Figure 20 and Figure 21.

In Figure 22, the test plane trajectories after using the three algorithms have been plotted on Google Earth. The brown line indicates only using ZUPT algorithm, the blue line indicates using ZUPT + iHDE, while the magenta line indicates using ZUPT + proposed heading constraint algorithm. As shown in Figure 22, the magenta line is closer to the actual trajectory of the pedestrian, while the blue and yellow lines deviate from the actual trajectory of the pedestrian. Therefore, compared to the existing iHDE method, the proposed method can have a better effect on the heading constraint of the trajectory's heading.

E. THE HEIGHT UPDATE ALGORITHM EXPERIMENT

Since test route 1 included stairs, pedestrians could go up and down stairs, and walk on a plane, which can effectively evaluate the effectiveness of the height update algorithm proposed in this paper. At the same time, as a comparison, the height correction method HUPT (height update algorithm) used in literature [19] also been analyzed in this section.

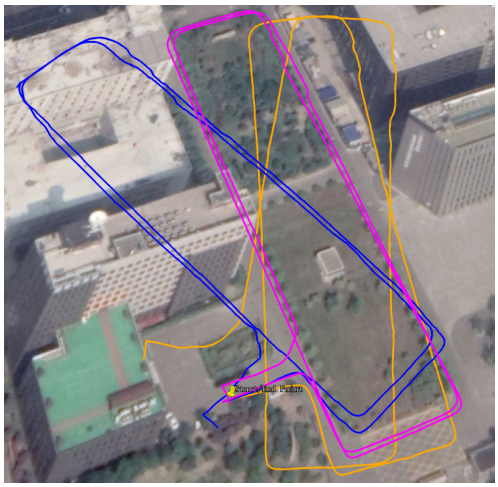

FIGURE 22. Pedestrian test plane projection trajectory on Google Earth. The brown line indicates only using ZUPT algorithm, the blue line indicates using ZUPT +iHDE (the method used in literatures), while the magenta line indicates using ZUPT + proposed heading constraint algorithm.

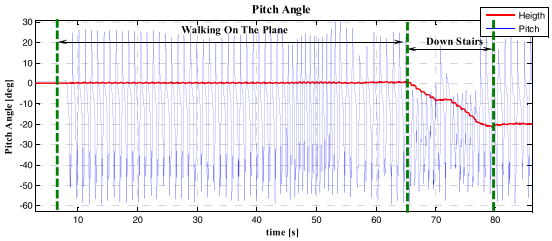

FIGURE 23. The variable of pitch angle during pedestrian normal walking and going downstairs.

In literature [19], it mainly uses the pitch angle to determine whether the pedestrian is walking on the plane or stairs, while we propose using the slope between adjacent one/several footsteps to determine the current state of pedestrians. If pedestrian walks on the plane, the height of current step is kept same to the previous footstep, which is same to method used in literature [19]. However, when pedestrian walks on the stairs, we proposed using the slope of the stairs to calculate the height change of the current footstep to constrain the height divergence, while in literature [19] and most other relative literatures, there is no correction method when pedestrian walks on stairs.

The experimental data collection process is as follows: the pedestrian started movement from point A of Floor 1, walked along the corridor, went around in C2, then returned to the corridor, kept walking until reached point B, went down the stairs from S2, and arrived at point E of Floor 0. On Floor 0, similarly to Floor 1, the pedestrian walked along the corridor, then walked around in C1, went upstairs through S1, and finally arriving at the starting point A of Floor1. The whole process repeated three times. At last, pedestrian still returned to point A of Floor1.

First, the relationship between the pitch angle and the height change during the whole pedestrian movement has been analyzed. Just as shown in the Figure 23 and Figure 24.

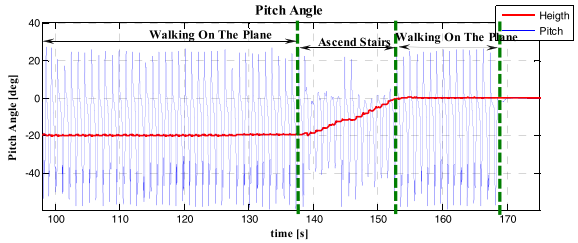

FIGURE 24. The variable of pitch angle during pedestrian normal walking and going upstairs.

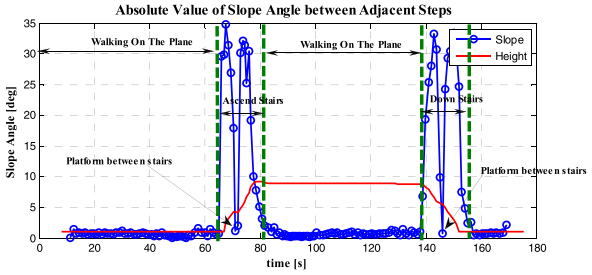

FIGURE 25. The absolute value of slope angle during pedestrian normal walking and going upstairs and downstairs.

In Figure 23 and Figure 24, the blue line indicates the change in pitch angle during the pedestrian's movement, and the red line indicates the height change of the pedestrian. As we can see, the change range of the pitch angle is different between the stairs and normal walking. However, the difference is not a reliable detector, especially when pedestrian under different motion modes (walking, running, etc.), the range of the pitch angle will change drastically. Also, the pitch angle of the inertial recursion inherently has errors, directly using them to determine whether a pedestrian is walking on horizontal surfaces or stairs is prone to errors.

Therefore, we proposed using the slope angle between adjacent footsteps. The absolute value of slope angle between adjacent footsteps is shown in Figure 25. The blue line indicates the absolute value of slope angle between adjacent footsteps, and the red line indicates the height change of the pedestrian's movement.

As we can see, when pedestrian walks on the plane, the absolute slope angle is close to zero degree, while walks on a staircase, the slope angle is significantly greater than zero, and its change range is between 5 and 35 degrees. Although actual slope angle of the experiment's stair is 30 degrees, the slope angle during staircase is not always close to 30 degrees due to the inertial recursion inherently has errors. Besides, during the staircase, the lowest value of slope angle (approximately zero degree) is because pedestrian walks on the platform between stairs which is a horizontal surface. Therefore, the slope angle between adjacent footsteps is a reliable detector to determine whether the pedestrian is walking on horizontal surfaces or stairs.

In the proposed height update algorithm of this paper, due to the inertial recursion inherently errors, for insurance, only when absolute value of the slope angle is greater than

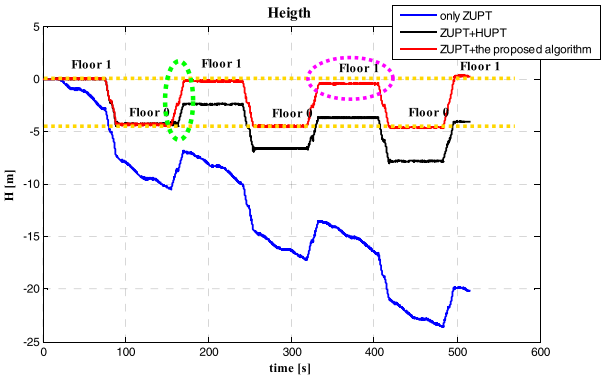

FIGURE 26. The height result during pedestrian movement. The blue line indicates only using ZUPT algorithm, the black line indicates using ZUPT +HUPT (the method used in literatures), while the red line indicates using ZUPT + the proposed height update algorithm. The yellow lines are the actual height of the floors.

20 degrees, the current step k is considered to be walking on the stairs. Then using the staircase correction algorithm in section IV revises the height error during staircase. Similarly, while pedestrian walks on the plane, using the horizon correction algorithm in section IV revises the height error.

In Figure 26, the height result during the whole pedestrian movement has been shown. And, three algorithms have been evaluated. The blue line indicates only using ZUPT algorithm, the black line indicates using ZUPT +HUPT (the method used in literature [19]), while the red line indicates using ZUPT + proposed height update algorithm. The yellow lines are the actual height of the floors. As we can see, when only using the ZUPT algorithm, the height dramatically diverges to −20m due to ZUPT algorithm mainly used to revise the velocity and has no effect on height correction. When using ZUPT+HUPT algorithm, the height can be effectively revised, especially when pedestrian walking on the horizon surface, the height almost keeps the same value (see the black line in Figure 26). However, when pedestrian walking on the stairs, as the HUPT method don't has any correction, the height has diverged during this stage. As shown in the green dotted oval, the height of the black line has not been corrected during the stairs, so after the pedestrian returns to the Floor 1, the height diverges to about −2m, while it actually should be 0m. Moreover, when pedestrian ends the movement, the height already diverges to −4m. When using ZUPT+ proposed height update algorithm, no matter pedestrian walking on the horizontal surface or stairs, the height can be effectively revised. The height results are close to the true results. Besides, in the proposed height update method, the staircase correction algorithm is used only when the slope angle is greater than 20 degrees. So, in the pink dotted oval, when pedestrian returns to Floor 1, the height slightly deviates from 0m.

In Figure 27, the relationship between absolute value of slope angle and height changes during the whole pedestrian movement has been shown. As we can see, the slope angle can be effectively used as the detector of the height change.

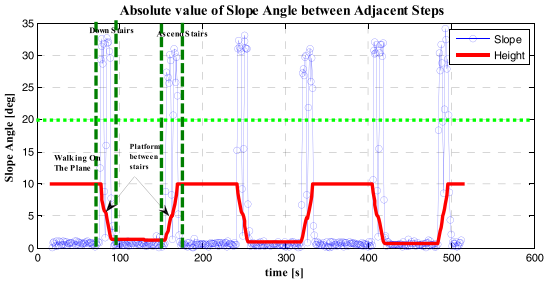

FIGURE 27. The relationship between absolute value of slope angle and height changes.

When pedestrian walks on the plane, the absolute value of slope angle is clearly close to 0 degree, while walks on the stairs, the slope angle is significantly greater than 0 degree. Due to errors in inertial recursion results, although the actual slope angle of the experiment's stair is 30 degrees, the slope angle during staircase (see Figure 27) is not always close to 30 degrees. Therefore, for insurance, in the proposed method, the staircase correction algorithm is used only when the slope angle is greater than 20 degrees. Furthermore, in order to reduce the effect of the inertial recursion error and improve the effectiveness of the slope angle as a detector of height change, the slope angle between adjacent multiple footsteps can calculated. The effectiveness of this method will be described in the next work.

VI. CONCLUSION

In this paper, three improved constraint algorithms have been proposed. Firstly, for the problem of failed detection of the stationary phase in the dynamic pedestrian gait, a novel stationary phase detection method has been proposed. In experiment, comparing with the traditional method, the proposed method can detect the stationary phase of each gait cycle accurately under various pedestrian movement. Secondly, for the heading divergence problem, an improved HDE method is proposed, which uses the reference heading to calculate the estimate position at the current footstep, then uses the position error between the estimate position and the inertia recursive position to restrain the heading divergence. In experiment, compared with the traditional method, the proposed method can better constrain the heading to the correct angle. At last, for the problem of height divergence of INS-based PDR system, by using the slope between adjacent one/several footsteps, the state of pedestrians can be effectively determined. Then, the slope of the plane and stairs is used to restrict the height divergence. In experiment, the height divergence can be constraint obviously, especially when pedestrian walks on the staircases.

In the proposed height update algorithm of this paper, it mainly used the slope angle between adjacent one footstep. So, the slope angle during staircase is not always close to the actual stair's slope due to the inertial recursion inherently has errors. In order to reduce the effect of the inertial recursion error and improve the reliability of the slope angle as a detector of height change, the slope angle between adjacent multiple footsteps can calculated. It will be described and evaluated in the future work.

REFERENCES

[1] L. Ojeda and J. Borenstein, "Personal dead-reckoning system for GPS-denied environments," in *Proc. IEEE Int. Workshop Saf., Secur. Rescue Robot.*, Sep. 2007, pp. 1–6.
[2] E. Foxlin, "Pedestrian tracking with shoe-mounted inertial sensors," *IEEE Comput. Grap. Appl.*, vol. 25, no. 6, pp. 38–46, Nov. 2005.
[3] J.-O. Nilsson, I. Skog, and P. Handel, "A note on the limitations of zupts and the implications on sensor error modeling," in *Proc. Int. Conf. Indoor Positioning Indoor Navigat. (IPIN)*, Sydney, NSW, Australia, Nov. 2012, pp. 13–15.
[4] S. K. Park and Y. S. Suh, "A zero velocity detection algorithm using inertial sensors for pedestrian navigation systems," *Sensors*, vol. 10, no. 10, pp. 9163–9178, Oct. 2010.
[5] Y. Wang and J. J. Wang, "A robust pedestrian navigation algorithm with low cost IMU," in *Proc. Int. Conf. Indoor Positioning Indoor Navigat. (IPIN)*, Sydney, NSW, Australia, Nov. 2012, pp. 1–7.
[6] M. Romanovas, V. Goridko, A. Al-Jawad, M. Schwaab, M. Traechtler, L. Klingbeil, and Y. Manoli, "A study on indoor pedestrian localization algorithms with foot-mounted sensors," in *Proc. Int. Conf. Indoor Positioning Indoor Navigat. (IPIN)*, Sydney, NSW, Australia, vol. 15, Nov. 2012, pp. 1–10.
[7] I. Skog, P. Handel, J. O. Nilsson, and J. Rantakokko, "Zero-velocity detection—An algorithm evaluation," *IEEE Trans. Biomed. Eng.*, vol. 57, no. 11, pp. 2657–2666, Nov. 2010.
[8] X. Meng, S. Sun, L. Ji, J. Wu, and W. Wong, "Estimation of center of mass displacement based on gait analysis," in *Proc. Int. Conf. Body Sensor Netw.*, Dallas, TX, USA, May 2011, pp. 150–155.
[9] C. Fischer, P. T. Sukumar, and M. Hazas, "Tutorial: Implementing a pedestrian tracker using inertial sensors," *IEEE Pervas. Comput.*, vol. 12, no. 2, pp. 17–27, Apr. 2013.
[10] K. Abdulrahim, C. Hide, T. Moore, and C. Hill, "Integrating low cost IMU with building heading in indoor pedestrian navigation," *J. Global Positioning Syst.*, vol. 10, no. 1, pp. 30–38, Oct. 2011.
[11] M. Benoussaad, B. Sijobert, K. Mombaur, and C. A. Coste, "Robust foot clearance estimation based on the integration of foot-mounted IMU acceleration data," *Sensors*, vol. 16, no. 1, p. 12, Dec. 2015.
[12] R. F. Alonso, E. Z. Casanova, and J. G. García-Bermejo, "Pedestrian tracking using inertial sensors," *J. Phys. Agents*, vol. 3, no. 1, pp. 35–43, Apr. 2016.
[13] K. Abdulrahim, C. Hide, T. Moore, and C. Hill, "Aiding MEMS IMU with building heading for indoor pedestrian navigation," in *Proc. Ubiquitous Positioning Indoor Navigat. Location Based Service (UPINLBS)*, Kirkkonummi, Finland, Oct. 2010, pp. 1–6.
[14] A. Jiménez, F. Seco, J. Prieto, and J. Guevara, "Indoor pedestrian navigation using an INS/EKF framework for Yaw drift reduction and a foot-mounted IMU," in *Proc. 7th Workshop Positioning Navigat. Commun. (WPNC)*, Dresden, Germany, Mar. 2010, pp. 135–143.
[15] S. Godha, G. Lachapelle, and M. E. Cannon, "Integrated GPS/INS system for pedestrian navigation in a signal degraded environment," in *Proc. 19th Int. Tech. Meeting Satellite Division Inst.-Navigat. (ION GNSS)*, Ft Worth, TX, USA, Sep. 2006, pp. 2151–2164.
[16] M. Ma, Q. Song, Y. Gu, and Z. Zhou, "Use of magnetic field for mitigating gyroscope errors for indoor pedestrian positioning," *Sensors*, vol. 18, no. 8, p. 2592, Aug. 2018.
[17] X. Cui, Y. Li, and Q. Wang, "Three-axis magnetometer calibration based on optimal ellipsoidal fitting under constraint condition for pedestrian positioning system using foot-mounted inertial sensor/magnetometer," in *Proc. IEEE/ION Position, Location Navigat. Symp. (PLANS)*, Monterey, CA, USA, Apr. 2018, pp. 166–174.
[18] A. R. Jimenez, F. Seco, and F. Zampella, "Improved heuristic drift elimination (iHDE) for pedestrian navigation in complex buildings," in *Proc. Int. Conf. Indoor Positioning Indoor Navigat. (IPIN)*, 2011, pp. 1–8.
[19] E. M. Diaz, S. Kaiser, D. B. Ahmed, "Height error correction for shoe-mounted inertial sensors exploiting foot dynamics," *Sensors*, vol. 18, p. 888, Mar. 2018.
[20] K. Abdulrahim, C. Hide, T. Moore, and C. Hill, "Using constraints for shoe mounted indoor pedestrian navigation," *J. Navigat.*, vol. 65, no. 1, pp. 15–28, Jan. 2012.

[21] L. Nguyen, H. M. La, and T. H. Duong, "Dynamic human gait phase detection algorithm," in *Proc. ISSAT Int. Conf. Modeling Complex Syst. Environ.*, Da Nang, Vietnam, Jun. 2015, pp. 1–5.
[22] W. Zhang, D. Wei, and H. Yuan, "Novel drift reduction methods in foot-mounted PDR system," *Sensors*, vol. 19, no. 18, p. 3962, Sep. 2019.
[23] M. Ma, Q. Song, Y. Gu, Y. Li, and Z. Zhou, "An adaptive zero velocity detection algorithm based on multi-sensor fusion for a pedestrian navigation system," *Sensors*, vol. 18, no. 10, p. 3261, Sep. 2018.
[24] X. Tian, J. Chen, Y. Han, J. Shang, and N. Li, "A novel zero velocity interval detection algorithm for self-contained pedestrian navigation system with inertial sensors," *Sensors*, vol. 16, no. 10, p. 1578, Sep. 2016.

WENCHAO ZHANG received the B.S. degree in surveying engineering from the China University of Mining and Technology (CUMT), in 2013, and the M.S. degree in surveying engineering from the Information Engineering University, in 2016. He is currently pursuing the Ph.D. degree in signal and information processing with the University of Chinese Academy of Sciences (UCAS).

He is also with the Aero Information Research (AIR) Institute, Chinese Academy of Science (CAS). His research interests include multiinformation fusion method, integrated navigation algorithm, pedestrian autonomous positioning algorithm based on MEMS sensors, and pedestrian indoor positioning method based on inertial sensors.

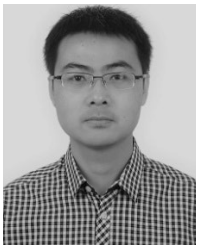

DONGYAN WEI received the B.S. degree in communication engineering from the University of Electronic Science and Technology of China (UESTC), in 2006, and the Ph.D. degree in signal and information processing from the Beijing University of Post and Telecommunication (BUPT), in 2011.

He is currently a Research Fellow of the Aero Information Research (AIR) Institute, Chinese Academy of Science (CAS). He is the author of one book, more than 30 articles, and more than 20 inventions. His research interests include indoor position, multisensor fusion, and Positioning in wireless networks.

Dr. Wei is a TPC member of the IPIN 2019 and the Deputy Chair of the IPIN 2020.

HONG YUAN received the Ph.D. degree from the Shanxi Observatory of the Chinese Academy of Sciences, in 1995.

From 1995 to 2004, he worked at the Wuhan Institute of Physics and Mathematics, Chinese Academy of Sciences. In 2004, he was transferred to the Academy of Opto-Electronics (AoE), Chinese Academy of Sciences. For many years, he has been engaged in research on ionospheric radio wave propagation, GPS, Beidou satellite navigation system construction, manned space applications, ionospheric physics, and ionospheric detection. He has hosted or participated in 13 national and provincial level projects, eight provincial and ministerial science and technology awards, more than 30 invention patents, and has published more than 60 articles. He is currently a Research Fellow of the Aero Information Research (AIR) Institute, Chinese Academy of Science. He is currently engaged in software and hardware design and algorithm research related to satellite navigation, multisource fusion navigation, and ionospheric detection.